Seismic evidence for lithospheric modification beneath the Mojave Neovolcanic Province, Southern California

Chelsea M. Allison,[1] Ryan C. Porter,[2] Matthew J. Fouch,[2] and Steven Semken[1]

Received 31 July 2013; revised 23 September 2013; accepted 25 September 2013; published 10 October 2013.

[1] The Mojave Neovolcanic Province (MNVP), located in the Mojave block of southern California, comprises late Miocene to Quaternary small-volume basaltic centers. Geochemistry indicates an asthenospheric source for the MNVP beginning in the late Miocene, but no physical evidence of missing mantle lithosphere has been presented. We utilize receiver functions and ambient noise tomography to image the lithosphere beneath the Mojave block. Regionally, we find thin crust that thickens distal to sites of MNVP volcanism. Shear wave velocities between 40 and 75 km depth are consistent with the presence of mantle lithosphere in the southern Mojave block and very thin or missing mantle lithosphere to the north. With one exception, MNVP volcanoes lie along this sharp boundary. Our observations, together with the established geologic history and geochemistry of the MNVP, can be explained by small-scale edge-driven convection producing ongoing lithospheric removal within the Mojave block. Our results provide another example of lithospheric instability that occurs in response to rapid changes in mantle dynamics induced by major changes in tectonic plate geometry.
Citation: Allison, C. M., R. C. Porter, M. J. Fouch, and S. Semken (2013), Seismic evidence for lithospheric modification beneath the Mojave Neovolcanic Province, Southern California, *Geophys. Res. Lett.*, *40*, 5119–5124, doi:10.1002/grl.50993.

1. Introduction

[2] The Mojave block lies within the southern Basin and Range and has a complex tectonic and magmatic history (Figure 1) related to Farallon plate subduction beneath North America. In the latest Paleogene, the Farallon spreading center was subducted and the margin evolved from a convergent margin to the present-day transform San Andreas Fault system [*Atwater*, 1970]. Regional calc-alkalic (arc-related) volcanism in the early Miocene (~25 Ma to 10 Ma) has been attributed to northward migration of the Mendocino triple junction [e.g., *Snyder et al.*, 1976]. As subduction ceased, volcanism across southern California transitioned to small basaltic fields in the late Miocene. This more recent (late Miocene to Quaternary) small-volume alkali basaltic volcanism, termed the Mojave Neovolcanic Province (MNVP) by *Glazner et al.* [1991], is geochemically associated with an asthenospheric mantle source [e.g., *Glazner et al.*, 1991; *Farmer et al.*, 1995]. The MNVP trends NW-SE and includes the Cima Volcanic Field (CVF) as well as Amboy and Pisgah craters [e.g., *Wise*, 1969]. Age estimates of the most recent flows of the CVF are as young as 10 ka [*Dohrenwend et al.*, 1984], while Amboy and Pisgah Craters are variously inferred to be Quaternary or Holocene based on morphology [*Glazner et al.*, 1991, and references within]. Petrological evidence suggests that younger (<5 Ma) MNVP basalts were not derived from lithospheric mantle sources and that they exhibit some contamination of mafic crust [e.g., *Glazner et al.*, 1991; *Farmer et al.*, 1995]. Many studies [e.g., *Glazner et al.*, 1991; *Farmer et al.*, 1995; *Leventhal et al.*, 1995] attribute the mantle source to inflow of asthenosphere through the slab window that opened as the Farallon spreading center subducted beneath North America.

[3] While detailed petrological and geochemical studies have provided significant constraints on the origin of the MNVP, early natural source seismic images of the lithosphere and asthenosphere [e.g., *Humphreys and Clayton*, 1990; *Humphreys and Dueker*, 1994] had resolution too coarse to provide detailed connections between MVNP volcanism and local structure, primarily due to limited station coverage within the Mojave Block. Previous work has also considered linkages between xenolith petrology and seismic reflection and refraction data collected in the 1960s and 1980s [e.g., *Wilshire et al.*, 1991]. In the past two decades, however, many new broadband seismic stations from permanent, regional, and transportable networks have been installed in the greater Mojave region. A number of recent studies have generated new images of the western U.S. crust and uppermost mantle using many of these data [e.g., *Yang and Ritzwoller*, 2008; *Bensen et al.*, 2009; *Lin et al.*, 2010; *Lekic et al.*, 2011; *Rau and Forsyth*, 2011; *Gilbert*, 2012; *Levander and Miller*, 2012], but a focused seismic study of the crust and mantle in this region is necessary to tie the chemical nature of past MNVP eruptions with the present-day physical setting.

[4] In this study, we used receiver function imaging techniques (H-κ and Common Conversion Point (CCP) stacking) and ambient noise tomography to image the crust and uppermost mantle beneath the MNVP. Our results demonstrate that intracrustal low-velocity zones exist in most of the study area, that the mantle lithosphere is missing beneath much of the Mojave Block, and that an isolated remnant lithospheric fragment remains beneath the southern MNVP. Placed in context with known geologic history and petrologic constraints, we suggest that small-scale convection along the edge of mantle lithosphere is a viable conceptual model that links the

Additional supporting information may be found in the online version of this article.

[1]School of Earth and Space Exploration, Arizona State University, Tempe, Arizona, USA.
[2]Department of Terrestrial Magnetism, Carnegie Institution of Washington, Washington, District of Columbia, USA.

Corresponding author: C. M. Allison, School of Earth and Space Exploration, Arizona State University, Tempe, AZ 85284, USA. (cmalliso@asu.edu)

0094-8276/13/10.1002/grl.50993

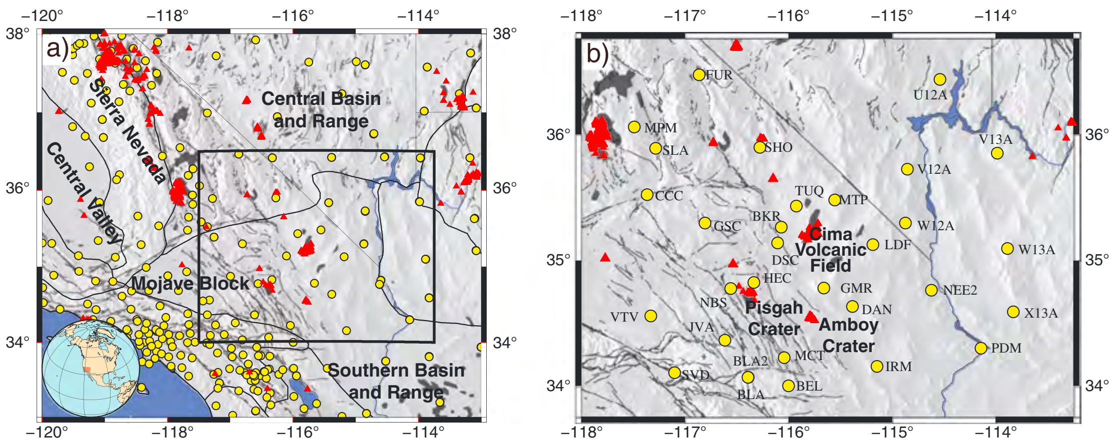

Figure 1. Study area. Red triangles denote volcanism with eruptive ages of 3 Ma and less from North American Volcanic and Intrusive Rock Database (NAVDAT) (http://www.navdat.org/; downloaded 06/2012); gray areas are volcanic rock from *Schruben et al*. [1994]. (a) Regional study area. Symbols show all regional broadband station locations. (b) Focused study area. Symbols show RF station locations.

petrologic and geophysical constraints for the MNVP, and can be extended to many regions of the western U.S. where recently destabilized lithosphere abounds.

2. Data and Methods

[5] We used receiver function (RF) analysis to image intracrustal interfaces, crustal thickness, and V_p/V_s across the region. Here we summarize our data and methods; see the supporting information for further details. We estimated radial and transverse RFs for each source-receiver pair using the iterative time domain deconvolution method of *Ligorria and Ammon* [1999]. We used a Gaussian width parameter of 2.5, which results in a pulse width of ~1 s (~2 s dominant period) yielding a depth resolution of ~3.5 km [e.g., *Eagar et al.*, 2011]. We trace edited and postprocessed the RFs using the MATLAB-based toolbox FuncLab [*Eagar and Fouch*, 2012].

[6] We used high quality RFs in single station (H-κ) and Common Conversion Point (CCP) stacking. We estimate the depth to Moho (H) and V_p/V_s ratio (κ) beneath each seismic station in the H-κ stacking method [*Zhu and Kanamori*, 2000] using the best-fitting values in the tradeoff between H and κ. This method does not perform well for some stations, mainly due to reverberations from deep basins. In those cases (eight stations), we evaluated the best-fitting Moho depth corresponding to the Ps arrival and crustal reverberations. To compute CCP stacks for regional correlations in structure, we back projected RF amplitudes along each source-receiver ray path using the Tectonic North America 1-D velocity model [*Grand and Helmberger*, 1984] as modified by *Eagar et al*. [2011].

[7] We used ambient noise tomography (ANT) to calculate shear velocities for the crust and upper mantle of the Mojave and surrounding region. ANT is based on the principle that the cross correlation of seismic noise recorded concurrently at two stations approximates the Green's function between the two stations. We used 1 Hz continuous vertical component data from all broadband stations archived at the Incorporated Research Institutions for Seismology Data Management Center (IRIS DMC) from 2005 through 2008 to coincide with the deployment of the EarthScope USArray Transportable Array in the region. We determined interstation phase velocities from the interstation cross correlations at periods from 8 to 40 s using the method described by *Bensen et al*. [2007]. We calculated 2-D phase velocity grids at different periods using the method of *Barmin et al*. [2001] with grid points located every 0.1°. We inverted these phase velocities, calculated at each grid point, for shear velocity using the code *surf* [*Herrmann*, 1987], with a constant-velocity starting model to produce a 3-D shear velocity model for the region.

3. Results

[8] We present the results of the RF and ANT analyses in Figures 2 and 3, and in Figures S3–S5 in the supporting information. We note that results from stations used in the RF analysis can be divided into three groups based upon features identified in radial RFs (Figure S3) detailed in the supporting information. Based on sensitivity kernels calculated for the starting model, we interpret shear velocities down to 80 km depth.

[9] We present map views of RF single station analysis and ANT results in Figures 2 and S4. These results show that the Moho is shallow (23–32 km) throughout this region and shallowest (≤25 km) in a zone near the CVF and Pisgah Crater (Figure 2a). For stations where H-κ analysis could be performed, V_p/V_s values are elevated (~1.8–2.0) for stations with thinner crust (i.e., near the CVF and Pisgah Crater) or near the San Andreas Fault, but normal (~1.75) for remaining stations, including those near Amboy Crater. In the uppermost crust (0–6 km), the ANT models show a zone of locally reduced velocities (<3.2 km/s) beneath Amboy Crater (Figure 2b). The region of thinned crust is also evident in ANT depth slices ranging from 22 km to 34 km, where locally increased velocities (>4.1 km/s) near the CVF and Pisgah Crater denote a shallower Moho. In the uppermost mantle (~40–75 km), both the CVF and Pisgah Crater lie along the SW-NE transition between lower shear wave velocities (4.2–4.4 km/s) to the NW and higher velocities (4.6–4.7 km/s) to the SE, while Amboy Crater is situated within the higher velocity region.

[10] In Figure 3, we display cross-sectional views of our RF CCP and ANT results. The CCP sections (Figures 3b–3d) show a clear and well-defined Moho with depths consistent

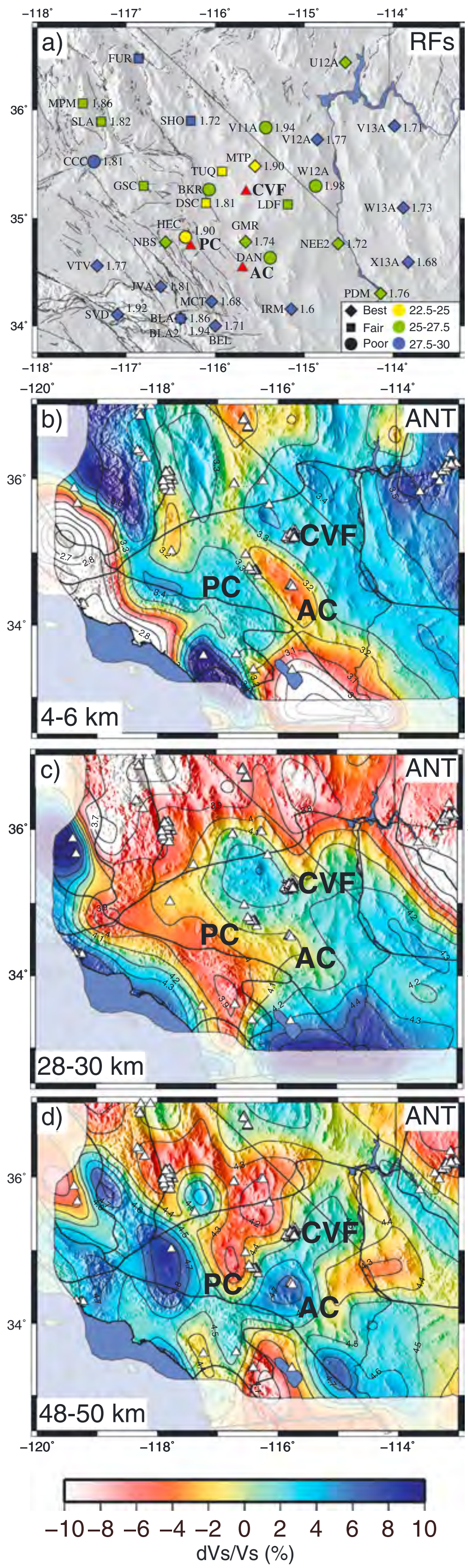

Figure 2. Map (plan) views of results. AC = Amboy Crater, CVF = Cima Volcanic Field, PC = Pisgah Crater. (a) Ps radial receiver function (RF) results. Colors denote crustal thickness inferred from H-κ analysis or moveout plot, while symbols denote quality of RFs (see supporting information for details). Numbers indicate V_p/V_s values for those stations with robust H-κ stacks. (b–d) Ambient noise tomography (ANT) results for various depth slices with depth range shown in lower left corner of map. Colors represent % perturbation from average layer model; contours annotate V_s in 0.1 km/s intervals. White triangles denote volcanism with eruptive ages of 3 Ma and less from NAVDAT (http://www.navdat.org/; downloaded 06/2012).

with H-κ results across the MNVP, with the shallowest (~25 km) Moho closest to the CVF and no deeper than 30 km depth. Some of the step-like changes over short (<10 km) lateral scales may be due to spatial smoothing artifacts, but these do not modify the overall observations or interpretations. The CCP images also show strong intracrustal negative amplitude arrival at 10–15 km depth that is pervasive throughout much of the region except beneath MNVP volcanic centers. The ANT results (Figures 3e–3g) show similar Moho depth variations and intracrustal features as the CCP model, although the inherent depth resolution of is less than that for CCP imaging. Beneath the crust, the ANT results show clear variations in mantle lithospheric structure. We find a distinct high velocity (4.6–4.7 km/s) region to the SE of the MNVP from 30 to 75 km depth (Figures 3e–3g), while to the northwest, we observe lower velocities (4.2–4.4 km/s; Figure 3f). The CVF and Pisgah Crater are located at the transition between these higher and lower velocity regions (Figure 3e), where the base of the higher velocity region sits at ~50 km depth (Figure 3g), increasing to ~75 km depth to the southeast (Figure 3f).

4. Lithospheric Evolution of the MNVP and Surrounding Region

[11] The results of this study enable a holistic examination of the present-day seismic velocity character of the broader MNVP region and its relationship with the regional geologic history. The intracrustal negative amplitude arrival (see Figures 3b–3d) is strong and sharp, consistent with the presence of a low-velocity zone (LVZ). This LVZ is pervasive throughout much of the area, including Amboy Crater, but is noticeably weak or absent beneath the CVF and Pisgah Crater. Our favored explanation of this structure and the surrounding LVZ is that melt has drained in areas of the crust without the LVZ as a result of recent volcanism. Implicit in this hypothesis is the presence of small volumes of intracrustal partial melt beneath other parts of the greater MNVP region. The notion of a melt drainage zone, similar to the scenario proposed by *Eagar et al.* [2011] for the High Lava Plains of Oregon, can be supported by observations of a locally shallower Moho with elevated V_p/V_s values, as expected for a crust that has been magmatically modified. In our study area, most areas with an intracrustal LVZ exhibit nominal crustal V_p/V_s values, suggesting that if the LVZ is due to partial melt, it must be focused in a very thin and sharp layer that does not substantially increase bulk V_p/V_s as expected for large volumes of partial melt. Forward modeling shows that a 5 km-thick low-velocity, high V_p/V_s layer can

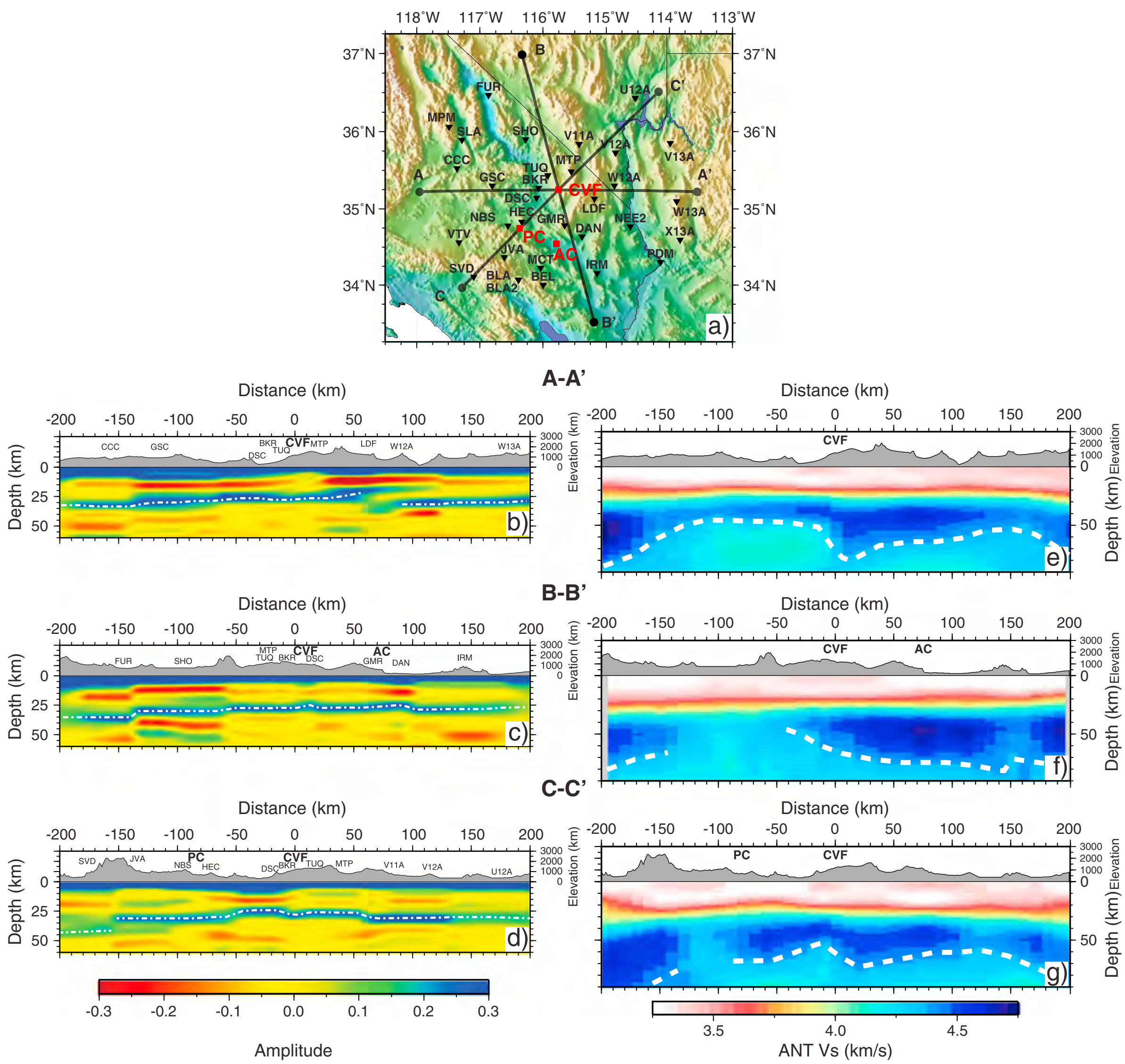

Figure 3. Cross-sectional views of results; vertical exaggeration on top topography panels only. AC = Amboy Crater, CVF = Cima Volcanic Field, PC = Pisgah Crater. Key RF stations labeled on Common Conversion Point (CCP) cross sections near topography. (a) Locations of cross sections are shown. (b–d) RF CCP stacking results. Colors denote relative amplitudes; blue is positive, and red is negative. Dashed lines represent interpreted Moho. (e–g) ANT results. Colors denote V_s in km/s. Dashed lines represent interpreted base of mantle lithosphere.

produce both the negative Ps conversion and an average whole-crust V_p/V_s ratio observed in receiver functions (see supporting information). A model including small volumes of partial melt in the crust is also consistent with elevated heat flow values, which are ~75–100 mW/m^2 nearest the study region [*Sass et al.*, 1994; U.S. Geological Survey heat flow database (http://earthquake.usgs.gov/research/borehole/heatflow/map.php, accessed 07/2013)]. Finally, we note that the crust beneath Amboy Crater contains a zone of reduced velocities in the uppermost crust (Figure 2b), is slightly thicker (~26 km), and exhibits a typical V_p/V_s crustal value of 1.74 (Figure 2a), denoting differences between the crust beneath Amboy Crater compared to the CVF and Pisgah Crater.

[12] In the uppermost mantle, differences among these eruptive centers also exist. Shear wave velocities throughout the entire study region are relatively low (4.2–4.7 km/s) but are consistent with a transition from uppermost mantle lithosphere to asthenosphere [e.g., *James et al.*, 2004]. A clear reduction in mantle velocities to asthenospheric values occurs at depths ranging from ~50 km to ~80 km across the region, suggesting that a laterally varying lithosphere-asthenosphere boundary exists. *Lekic et al.* [2011], *Rau and Forsyth* [2011], and *Levander and Miller* [2012] support this variation with evidence independent of our study. We can therefore infer that the CVF and Pisgah Crater lie directly on the boundary (most clearly observed in Figure 2d) between lithosphere to the SE and asthenosphere to the NW. Amboy Crater, however, is situated atop a parcel of thin, but distinct, mantle lithosphere in the southern portion of the southern Mojave block.

[13] Two plausible mechanisms may explain the observed differences in lithospheric structure beneath the Mojave block: preferential lithospheric thinning and lithospheric delamination. In general, both processes may result from relatively recent extension, hydration of the overriding plate during

subduction, inherent differences in lithospheric strength or thickness, or a response to rapid asthenospheric inflow as regional subduction terminated. While it remains a challenge to fully distinguish between these processes, we can use known geological constraints from the Cenozoic evolution of the Mojave block to work toward a viable model.

[14] Widespread extension in the Mojave Block during the early Miocene, which ceased at ~18 Ma [e.g., *Glazner et al*., 2002], may have led to thinned lithosphere. The first silicic eruptive centers in the region appeared at this time, while the basaltic MNVP centers emerged later. Although the timing of these events is consistent with extension that produces a suite of volcanism in the Mojave block, an additional influence, such as significant differences in inherent lithospheric strength or thickness during the middle Miocene or preferential hydration of focused lithospheric zones, is necessary to reconcile the present-day existence of the southern lithospheric fragment. We note that the lithospheric boundary closely follows the Mojave block miogeoclinal-cratonal hinge line (MCH) [e.g., *Martin and Walker*, 1992; *Glazner et al*., 2002], which represents a Proterozoic lithospheric boundary [*Miller et al*., 2000]. In a preferential lithospheric thinning scenario, extensional stresses could focus on the younger lithosphere to the west while leaving the older lithospheric package relatively intact.

[15] Alternatively, lithospheric delamination could remove mantle lithosphere and perhaps the lowermost crust throughout the MNVP. As the lithosphere peels away, small-scale edge-driven convection would continue to erode the mantle lithosphere from the northwest. This process has been proposed for other regions underlain by a significant step in lithospheric thickness, such as the Sierra Nevada range to the west of the MNVP [e.g., *Manley et al*., 2000], the Big Pine Volcanic Field to the north [*Gazel et al*., 2012], and the Colorado Plateau to the east [e.g., *van Wijk et al*., 2010; *Levander et al*., 2011; *Reid et al*., 2012]. In this conceptual model, delamination is initiated during the opening of the Farallon slab window [e.g., *Farmer et al*., 1995], perhaps instigated by a shift in the stress regime with the cessation of widespread extension at 18 Ma [*Glazner et al*., 2002], the sharp difference in lithospheric character near the MCH [e.g., *Miller et al*., 2000; *Levander and Miller*, 2012], or a combination of these processes.

[16] Lithospheric removal linked to the opening of the Farallon slab window is therefore a straightforward model to explain the recent tectonics and volcanism within the MNVP and in surrounding regions [e.g., *Gazel et al*., 2012]. Volcanoes in the CVF are characterized by entrained mantle xenoliths, larger eruptive volumes, and less crustal contamination, compared to Pisgah and Amboy Craters, which perhaps had midcrustal melts pooled for a period of time prior to eruption [e.g., *Glazner et al*., 1991; *Farmer et al*., 1995]. Our results, along with this evidence, suggest that the CVF represents a more evolved zone in the lithospheric destruction process, whereas Pisgah continues to evolve at the lithospheric boundary, and the lithosphere around Amboy is still being modified. Amboy may therefore be one of multiple small basaltic centers that should appear locally as the Amboy lithospheric block continues to erode.

[17] In conclusion, while lithospheric modification and removal have been proposed as the cause of widespread Cordilleran tectonomagmatism in the middle Cenozoic [e.g., *Humphreys*, 1995], it is also an important factor in subsequent neotectonic and neomagmatic episodes [e.g., *Zandt et al*., 2004; *Hales et al*., 2005; *West et al*., 2009; *Levander et al*., 2011; *Gazel et al*., 2012; *Levander and Miller*, 2012]. It may prove to be the rule rather than the exception during ongoing tectonic evolution of the western U.S., and more broadly, regions where rapid changes in mantle dynamics occur. Further multidisciplinary and coordinated study is necessary to examine the timing of such events in the volcanic record and carefully examine their links to geochemical, petrological, and seismological constraints on broader, continental-wide, scales.

[18] **Acknowledgments.** This work was supported by the National Science Foundation (grant EAR-1053317) and DTM. We appreciate the efforts of the EarthScope USArray Transportable Array and SCEC field teams in data collection, and the IRIS Data Management Center and SCEC Data Center for providing waveform data. We value FuncLab and receiver function evaluation training provided by Jonathan Delph. Thanks to Mark Stevens (ASU), Michael Acierno (DTM), and Sandy Keiser (DTM) for providing computer systems support.

[19] The Editor thanks two anonymous reviewers for their assistance in evaluating this paper.

References

Atwater, T. (1970), Implications of plate tectonics for the Cenozoic tectonic evolution of western North America, *Geol. Soc. Am. Bull.*, *81*, 3513–3536.

Barmin, M. P., M. H. Ritzwoller, and A. L. Levshin (2001), A fast and reliable method for surface wave tomography, *Pure Appl. Geophys.*, *158*, 1351–1375.

Bensen, G. D., M. H. Ritzwoller, M. P. Barmin, A. L. Levshin, F. Lin, M. P. Moschetti, N. M. Shapiro, and Y. Yang (2007), Processing seismic ambient noise data to obtain reliable broad-band surface wave dispersion measurements, *Geophys. J. Int.*, *169*, 1239–1260, doi:10.1111/j.1365-246X.2007.03374.x.

Bensen, G. D., M. H. Ritzwoller, and Y. Yang (2009), A 3-D shear velocity model of the crust and uppermost mantle beneath the United States from ambient seismic noise, *Geophys. J. Int.*, *177*, 1177–1196, doi:10.1111/j.1365-246X.2009.04125.x.

Dohrenwend, J. C., L. D. McFadden, B. D. Turrin, and S. G. Wells (1984), K-Ar dating of the Cima volcanic field, eastern Mojave Desert, California: Late Cenozoic volcanic history and landscape evolution, *Geology*, *12*, 163–167.

Eagar, K. C., and M. J. Fouch (2012), FuncLab: A MATLAB interactive toolbox for handling receiver function datasets, *Seismol. Res. Lett.*, *83*(3), 596–603, doi:10.1785/gssrl.83.3.596.

Eagar, K. C., M. J. Fouch, D. E. James, and R. W. Carlson (2011), Crustal structure beneath the High Lava Plains of eastern Oregon and surrounding regions from receiver function analysis, *J. Geophys. Res.*, *116*, B02313, doi:10.1029/2010JB007795.

Farmer, G. L., A. F. Glazner, H. G. Wilshire, J. L. Wooden, W. J. Pickthorn, and M. Katz (1995), Origin of late Cenozoic basalts at the Cima volcanic field, Mojave Desert, California, *J. Geophys. Res.*, *100*(B5), 8399–8415.

Gazel, E., T. Plank, D. W. Forsyth, C. Bendersky, C.-T. A. Lee, and E. H. Hauri (2012), Lithosphere versus asthenosphere mantle sources at the Big Pine Volcanic Field, California, *Geochem. Geophys. Geosyst.*, *13*, Q0AK06, doi:10.1029/2012GC004060.

Gilbert, H. (2012), Crustal structure and signatures of recent tectonism as influenced by ancient terranes in the western United States, *Geosphere*, *8*(1), 141–157, doi:10.1130/GES00720.1.

Glazner, A. F., G. L. Farmer, W. T. Hughes, J. L. Wooden, and W. Pickthorn (1991), Contamination of basaltic magma by mafic crust at Amboy and Pisgah Craters, Mojave Desert, California, *J. Geophys. Res.*, *96*(B8), 13,673–13,691.

Glazner, A. F., D. J. Walker, J. M. Bartley, and J. M. Fletcher (2002), Cenozoic evolution of the Mojave block of southern California, in *Geologic Evolution of the Mojave Desert and Southwestern Basin and Range*, Mem. Geol. Soc. Am., vol. 195, edited by A. F. Glazner et al., pp. 19–41, Geological Society of America, Boulder, Colorado.

Grand, S. P., and D. V. Helmberger (1984), Upper mantle shear structure of North America, *Geophys. J. R. Astron. Soc.*, *76*(2), 399–438.

Hales, T. C., D. L. Abt, E. D. Humphreys, and J. J. Roering (2005), A lithospheric instability origin for Columbia River flood basalts and Wallowa Mountains uplift in northeast Oregon, *Nature*, *438*, 842–845, doi:10.1038/nature04313.

Herrmann, R. B. (1987), Computer programs in seismology, St. Louis, Mo., St. Louis University.

Humphreys, E. D. (1995), Post-Laramide removal of the Farallon slab, western United States, *Geology*, *23*(11), 987–990.
Humphreys, E. D., and R. W. Clayton (1990), Tomographic image of the southern California mantle, *J. Geophys. Res.*, *95*(B12), 19,725–19,746.
Humphreys, E. D., and K. G. Dueker (1994), Western U.S. upper mantle structure, *J. Geophys. Res.*, *99*(B5), 9615–9634.
James, D. E., F. R. Boyd, D. Schutt, D. R. Bell, and R. W. Carlson (2004), Xenolith constraints on seismic velocities in the upper mantle beneath southern Africa, *Geochem. Geophys. Geosyst.*, *5*, Q01002, doi:10.1029/2003GC000551.
Lekic, V., S. W. French, and K. M. Fischer (2011), Lithospheric thinning beneath rifted regions of southern California, *Science*, *334*(6057), 783–787, doi:10.1126/science.1208898.
Levander, A., and M. S. Miller (2012), Evolutionary aspects of lithosphere discontinuity structure in the western U.S, *Geochem. Geophys. Geosyst.*, *13*, Q0AK07, doi:10.1029/2012GC004056.
Levander, A., B. Schmandt, M. S. Miller, K. Liu, K. E. Karlstrom, R. S. Crow, C.-T. A. Lee, and E. D. Humphreys (2011), Continuing Colorado plateau uplift by delamination style convective lithospheric downwelling, *Nature*, *472*, 461–466, doi:10.1038/nature10001.
Leventhal, J. A., M. R. Reid, A. Montana, and P. Holden (1995), Mesozoic invasion of crust by MORB-source asthenospheric magmas, U.S. Cordilleran interior, *Geology*, *23*(5), 399–402.
Ligorria, J. P., and C. J. Ammon (1999), Iterative deconvolution and receiver function estimation, *Bull. Seismol. Soc. Am.*, *89*(5), 1395–1400.
Lin, F.-C., M. H. Ritzwoller, Y. Yang, M. P. Moschetti, and M. J. Fouch (2010), Complex and variable crustal and uppermost mantle seismic anisotropy in the western United States, *Nat. Geosci.*, *4*, 55–61, doi:10.1038/NGEO1036.
Manley, C. R., A. F. Glazner, and G. L. Farmer (2000), Timing of volcanism in the Sierra Nevada of California: Evidence for Pliocene delamination of the batholithic root?, *Geology*, *28*(9), 811–814.
Martin, M. W., and J. D. Walker (1992), Extending the western North American Proterozoic and Paleozoic continental crust through the Mojave Desert, *Geology*, *20*, 753–756.
Miller, J. S., A. F. Glazner, G. L. Farmer, I. B. Suayah, and L. A. Keith (2000), A Sr, Nd, and Pb isotopic study of mantle domains and crustal structure from Miocene volcanic rocks in the Mojave Desert, California, *Geol. Soc. Am. Bull.*, *112*(8), 1264–1279.
Rau, C. J., and D. W. Forsyth (2011), Melt in the mantle beneath the amagmatic zone, southern Nevada, *Geology*, *39*(10), 975–978, doi:10.1130/G32179.1.
Reid, M. R., R. A. Bouchet, J. Blichert-Toft, A. Levander, K. Liu, M. S. Miller, and F. C. Ramos (2012), Melting under the Colorado Plateau, USA, *Geology*, *40*(5), 387–390, doi:10.1130/G32619.1.
Sass, J. H., A. H. Lachenbruch, S. P. Galanis Jr., P. Morgan, S. S. Priest, T. H. Moses Jr., and R. J. Munroe (1994), Thermal regime of the southern Basin and Range Province: 1. Heat flow data from Arizona and the Mojave Desert of California and Nevada, *J. Geophys. Res.*, *99*, 22,093–22,119.
Schruben, P. G., R. E. Arndt, W. J. Bawiec, P. B. King, and H. M. Beikman (1994), Geology of the Conterminous United States at 1:2,500,000 scale—A digital representation of the 1974 P.B. King and H.M. Beikman map, U.S. Geol. Surv. Digital Data Ser., Reston, VA.
Snyder, W. S., W. R. Dickinson, and M. L. Silberman (1976), Tectonic implications of space-time patterns of Cenozoic magmatism in the western United States, *Earth Planet. Sci. Lett.*, *32*, 91–106.
West, J. D., M. J. Fouch, J. B. Roth, and L. T. Elkins-Tanton (2009), Vertical mantle flow associated with a lithospheric drip beneath the Great Basin, *Nat. Geosci.*, *2*, 439–444, doi:10.1038/NGEO526.
van Wijk, J. W., W. S. Baldridge, J. van Hunen, S. Goes, R. Aster, D. D. Coblentz, S. P. Grand, and J. Ni (2010), Small-scale convection at the edge of the Colorado Plateau: Implications for topography, magmatism, and evolution of Proterozoic lithosphere, *Geology*, *38*(7), 611–614, doi:10.1130/G31031.1.
Wilshire, H. G., A. V. McGuire, J. S. Noller, and B. D. Turrin (1991), Petrology of lower crustal and upper mantle xenoliths from the Cima Volcanic Field, California, *J. Petrol.*, *32*, 169–200.
Wise, W. S. (1969), Origin of basaltic magmas in the Mojave Desert area, California, *Contrib. Mineral. Petrol.*, *23*, 53–64.
Yang, Y., and M. H. Ritzwoller (2008), Teleseismic surface wave tomography in the western U.S. using the Transportable Array component of USArray, *Geophys. Res. Lett.*, *35*, L04308, doi:10.1029/2007GL032278.
Zandt, G., H. Gilbert, T. J. Owens, M. Ducea, J. Saleeby, and C. H. Jones (2004), Active foundering of a continental arc root beneath the southern Sierra Nevada in California, *Nature*, *431*, 41–46, doi:10.1038/nature02847.
Zhu, L., and H. Kanamori (2000), Moho depth variation in southern California from teleseismic receiver functions, *J. Geophys. Res.*, *105*(B2), 2969–2980.